Asymmetric salt fingers induced by a nonlinear equation of state

Tamay M. Özgökmen and Oleg E. Esenkov
RSMAS/MPO, University of Miami, 4600 Rickenbacker Causeway, Miami, Florida 33149

(Received 28 October 1997; accepted 4 April 1998)

The impact of the nonlinearity in the equation of state associated with the change in the thermal expansion coefficient with temperature on the structure of fingers growing from an interface between two mixed layers is investigated using a numerical model. It is shown that the nonlinearity acts to enhance the buoyancy force acting on the descending fingers with respect to that acting on the ascending fingers, resulting in narrower and faster-growing descending fingers than ascending fingers. The results are discussed with emphasis on the vertical variability of properties along the fingers. © *1998 American Institute of Physics.* [S1070-6631(98)00408-5]

I. INTRODUCTION

Double-diffusive instabilities of a fluid rely on the presence of two state variables that diffuse at different rates. Finger instability can occur when the faster diffusing component makes a stabilizing contribution to the density gradient while the slower diffusing component makes a destabilizing contribution. With the overall stratification remaining stable, the structures realized are tall, narrow cells of alternatively rising and sinking fluid. In the original theory and experiment performed with a heat-salt system (Stern[1]), the two orders of magnitude difference between the diffusivities of salt and heat led to the near conservation of salt in narrow columns, hence the name ''salt fingers.''

Salt fingers obtained in laboratory experiments[2,3] are symmetric, i.e., sinking and rising columns have the same horizontal and vertical structure, the same wave number and the same growth rate. Analytical studies of salt fingers (e.g., Stern,[1] Schmitt,[4] Kunze[5]) as well as numerical simulations (Piacsek and Toomre,[6] Shen,[7,8] Özgökmen *et al.*[9]) have employed a linear equation of state, leading to a symmetric array of salt fingers. The impact of the nonlinearity in the equation of state on the finger interface was explored by McDougall,[10,11] who found in laboratory experiments that the nonlinearity causes the salt finger interfaces between mixed layers to migrate upward, an effect also observed by Schmitt.[12] In these experiments, the lower layer grew at the expense of the upper layer, indicating an asymmetry between the upward and downward fluxes. This behavior implies a possible asymmetry in the finger structure. Schmitt (personal communication) suggests that asymmetric fingers may result from the nonlinearities in the equation of state.

The purpose of this study is to explore the impact of the nonlinearity in the equation of state due to the change of the thermal expansion coefficient with temperature on the structure of salt fingers growing from a sharp interface between two mixed layers. The investigation is conducted using a numerical model, because the nonlinear term can readily be included in the model equations and its effect can be isolated. Unlike numerical experiments, the effect of a nonlinear term in the equation of state on the finger structure cannot easily be investigated in laboratory experiments. Analytical solutions are also difficult to obtain due to the nonlinearity.

The paper is organized as follows. In Sec. II we give physical reasons why a nonlinear equation of state should lead to asymmetric salt fingers. Section III describes the numerical model. The experimental setup is discussed in Sec. IV, and the numerical experiments are presented in Sec. V. Finally, the main results are summarized in the concluding section.

II. A MECHANISM FOR ASYMMETRY

The equation of state of seawater is nonlinear, and the sense of the nonlinearity is such that a mixture of two water masses of the same density but different temperatures and salinities is denser than the original water masses. This nonlinearity may be thought of as being primarily due to variation of the thermal expansion coefficient with temperature, and the following quadratic expression is a good approximation to the water density:[10]

$$\rho=\rho_0[1-\alpha(T-T_0)+\beta(S-S_0)-\gamma(T-T_0)^2], \qquad (1)$$

where ρ_0, T_0 and S_0 are the reference values of density, temperature and salinity, respectively. Density variations caused by temperature changes are represented by linear and nonlinear terms with corresponding expansion coefficients α and γ, while β is the linear contraction coefficient for salinity.

To understand the mechanism leading to vertical asymmetry in salt fingers, consider a simple case of two layers with different temperatures and salinities separated by a sharp interface (Fig. 1). If cold, fresh water is placed under a layer of warm, salty water, salt fingers can grow at the interface. After a short time compared to the diffusion time scale of salt, temperatures in the upward and downward growing fingers become, respectively,

$$T_u=T_2+\delta T,$$

$$T_d=T_1-\delta T,$$

where T_1 and T_2 are the temperatures of the upper and lower layers, respectively, and δT is the temperature change in the

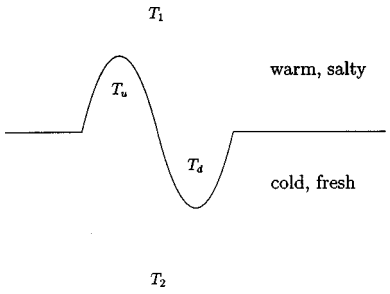

FIG. 1. Notations regarding a simple diagram of the onset of finger instability from a sharp interface between two mixed layers.

fingers due to the diffusion of temperature. It is assumed that δT is the same for both upward and downward growing fingers during the initial growth. If $\rho_u^{\rm lin}$ and $\rho_d^{\rm lin}$ contain contributions to the density of the fingers due to the linear part of the equation of state, the expressions for the densities of the disturbances can be written as:

$$\rho_u=\rho_u^{\rm lin}-\gamma(T_2+\delta T-T_0)^2,$$

$$\rho_d=\rho_d^{\rm lin}-\gamma(T_1-\delta T-T_0)^2.$$

The upward moving parcel experiences a buoyancy force proportional to $\Delta\rho_u=\rho_1-\rho_u$, while the force acting on the downward moving parcel is proportional to $\Delta\rho_d=\rho_d-\rho_2$ (both are defined as positive quantities), where

$$\rho_1=\rho^{\rm lin}(T_1,S_1)-\gamma(T_1-T_0)^2,$$

$$\rho_2=\rho^{\rm lin}(T_2,S_2)-\gamma(T_2-T_0)^2$$

are the densities of the upper and lower layers, respectively. After simple algebra we find that the difference in the magnitudes of the buoyancy forces acting on the downward and upward moving parcels is proportional to

$$\Delta\rho_d-\Delta\rho_u=2\gamma\delta T(T_1-T_2-\delta T). \tag{2}$$

The difference is larger than zero as long as δT is not equal to zero, or δT is not equal to T_1-T_2. In the finger zone, $\delta T<T_1-T_2$, and therefore the above equation states that the descending fingers are subject to a greater buoyancy forcing than the ascending fingers. The difference in buoyancy forces that sinking and rising fingers experience is entirely due to nonlinearity of the equation of state, and it disappears when $\gamma=0$. It will be shown by numerical experiments that this differential buoyancy forcing leads to asymmetric evolution of ascending and descending fingers.

III. THE NUMERICAL MODEL

The numerical model integrates the two-dimensional equations of motion of an incompressible fluid subject to the Boussinesq approximation. In order to reduce the number of parameters, the following nondimensionalization is used:

$$(x,z)=L(x^*,z^*);\quad \psi=\nu\psi^*;\quad t=\frac{L^2}{\nu}t^*;$$

$$T=\triangle TT^*;\quad S=\triangle SS^*.$$

Dropping stars, the prognostic equations for the conservation of vorticity, temperature, and salinity become

$$\zeta_t+J(\psi,\zeta)=\frac{\rm Ra}{\rm Pr}\left[T_x(1+\epsilon T)-\frac{S_x}{R_\rho^0}\right]+\nabla^2\zeta, \tag{3}$$

$$T_t+J(\psi,T)=\frac{1}{\rm Pr}\nabla^2T, \tag{4}$$

$$S_t+J(\psi,S)=\frac{1}{\rm Sc}\nabla^2S. \tag{5}$$

The stream function is calculated diagnostically from

$$\nabla^2\psi=\zeta. \tag{6}$$

Here ν is the kinematic viscosity, K_T and K_S are the respective diffusivities of temperature and salinity, $\triangle T$ and $\triangle S$ are the respective T and S differences across the vertical extent of the domain, g is the gravitational acceleration, and L is the width of the domain. The nondimensional parameters are the Prandtl number ${\rm Pr}=\nu/K_T$, the Schmidt number ${\rm Sc}=\nu/K_S$, the Rayleigh number based on temperature ${\rm Ra}=g\alpha\triangle TL^3/\nu K_T$, the nonlinearity parameter $\epsilon=2\gamma\triangle T/\alpha$, and the linear density ratio $R_\rho^0=\alpha\triangle T/\beta\triangle S$, whereas the actual (nonlinear) density ratio can be expressed as $R_\rho=R_\rho^0(1+\epsilon T)T_z/S_z$.

The prognostic equations (3)–(5) are advanced in time using a predictor-corrector type leapfrog method.[13] The time step is calculated at every iteration based on the maximum speed induced by diffusive and advective processes. The Jacobian operator $J(a,b)=a_xb_z-a_zb_x$ is computed using the formulation proposed by Arakawa[14] that conserves kinetic energy and entropy, while accurately maintaining the property $J(a,b)=-J(b,a)$. All other differential operators are approximated by using central differences. The diagnostic equation (6) is inverted using a fast Fourier transform solver.[15]

IV. THE EXPERIMENTAL SETUP

The purpose of the experiments in this study is to explore the behavior of rising and sinking fingers as a function of the nonlinearity in the equation of state, which is quantified by the parameter ϵ. A suitable experimental configuration for this purpose is a sharp interface sandwiched between two mixed layers (Fig. 2). The lower layer contains cold and fresh water ($T=S=0$), while the upper layer contains warm and salty water ($T=S=1$), consistent with the conditions for the salt finger instability. The reference temperature corresponds to the lower layer temperature ($T_0=0$). All experiments are conducted with a heat-salt system (${\rm Pr}=7$, ${\rm Sc}=700$). The additional requirement for salt finger instability is

$$1<R_\rho<K_T/K_S. \tag{7}$$

Here, the initial (model) density ratio is taken as $R_\rho=1.8$, and since $K_T/K_S={\rm Sc/Pr}=100$, the above requirement is satisfied. It is anticipated that a small density ratio (i.e., $R_\rho\rightarrow1$)

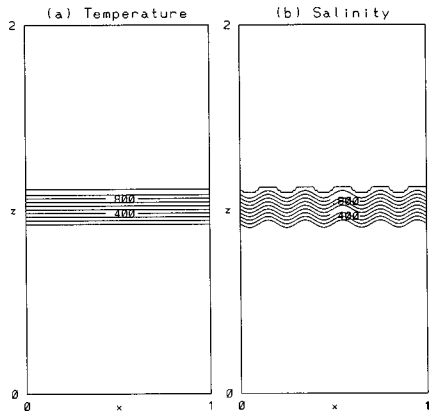

FIG. 2. Initial distributions for (a) temperature and (b) salinity fields. The contour interval is 0.1 in nondimensional units.

will result in a faster development of fingers than a large density ratio (i.e., $R_\rho \to K_T/K_S$), because the former is gravitationally less stable.

The following relation gives an approximate length scale of the fastest-growing fingers in the case of a linear equation of state (cf. Kunze[5]):

$$\frac{L}{\lambda} = \frac{1}{2\pi}\left[\frac{L}{h} Ra\left(1 - \frac{1}{R_\rho^0}\right)\right]^{1/4},$$

where λ is the wavelength of the fastest-growing fingers and h is the thickness of the salt finger interface. The Rayleigh number is $\mathrm{Ra} = 1 \times 10^6$ in these experiments. The thickness of the interface between the two layers is 20% of the horizontal extent of the domain. Hence, the above relationship yields six pairs of fingers. However, experiments carried out with five and seven pairs showed similar growth rates, while the growth rate decreased for smaller and larger wave numbers. For a better numerical resolution of the fingers, we opt to initialize the system with a perturbation with wave number 5. These perturbations are applied to salinity fields only (Fig. 2), because the temperature field diffuses quickly and eliminates the initial perturbations.

The integrations are carried out with a resolution of 201 grid points in each direction, so that the horizontal resolution of the fingers is approximately 20 points. In order to assure that this numerical resolution is sufficient for the purpose of the present study, lower resolution experiments are also performed with twice the grid spacing (not shown), which indicated essentially the same results as those discussed below. The aspect ratio of the domain is $L_z/L = 2$ to allow space in the vertical for the fingers to evolve. Hence, $\triangle z = 2\triangle x$ in order to take computational advantage of the finger shape. The parameters of the experiments are listed in Table I.

The boundary conditions on the left and right boundaries are periodic. At the top and bottom, the boundary conditions are free-slip and no vertical mass flux ($\zeta = 0$, $\psi_x = 0$). Furthermore, no heat and salt fluxes are allowed across these boundaries (i.e., $T_z = 0$, $S_z = 0$). These boundary conditions are preferred because they prevent any import or export of energy into the model domain during the evolution of the system. The integrations are terminated before the fingers interact with the vertical boundaries so that the effect of these boundaries on the interior dynamics is not significant.

TABLE I. The common parameters of the numerical experiments. Three experiments are conducted with $\epsilon = 0$, $\epsilon = 1$, and $\epsilon = 3$.

L	1
L_z	2
Pr	7
Sm	700
R_ρ	1.8
Ra	1×10^6
Resolution	201^2

V. NUMERICAL EXPERIMENTS

The initial evolution of fingers is explored as a function of the parameter ϵ. Three experiments are conducted with $\epsilon = 0$, $\epsilon = 1$, and $\epsilon = 3$. The first experiment incorporates a linear equation of state and serves as a reference case. In the second experiment, the contribution of the nonlinear term in the equation of state is as large as that of the linear term for temperature. Finally, in the third case, the nonlinear term dominates the linear term. Such large contributions of the nonlinear term can be achieved physically by increasing the temperature difference between the two layers, provided that the salinity difference is increased accordingly in order to preserve the density ratio. Laboratory experiments with a similar range of the nonlinearity parameter values have been carried out by McDougall.[10,11] A nonlinearity parameter of $O(1)$ can be obtained typically with a temperature difference of about 10–20 °C and a salinity difference of about 2%–5% between the upper and lower layers (for additional details on the laboratory setup, the reader is referred to McDougall[11]).

A. Growth of fingers

The density distributions corresponding to the initial conditions are illustrated for all three cases in Fig. 3. As the parameter ϵ increases, the stabilizing effect of temperature is enhanced and the interface becomes more stably stratified. Consequently, one can expect a slower evolution of fingers

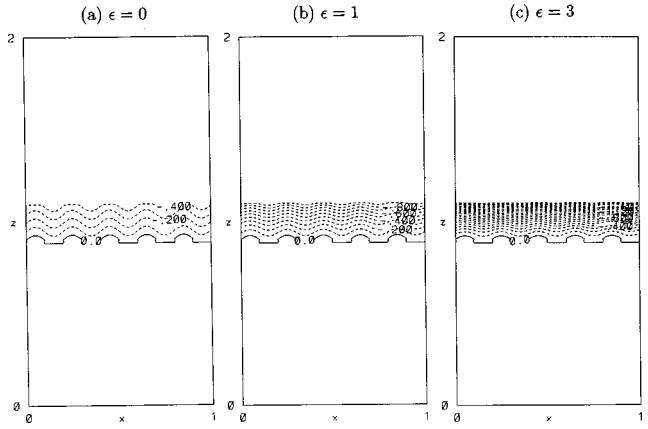

FIG. 3. Initial distributions of the nondimensional density $\rho = -T - (\epsilon/2)T^2 + S/R_\rho$ for experiments with (a) $\epsilon = 0$, (b) $\epsilon = 1$, (c) $\epsilon = 3$ (CI $= 0.1$).

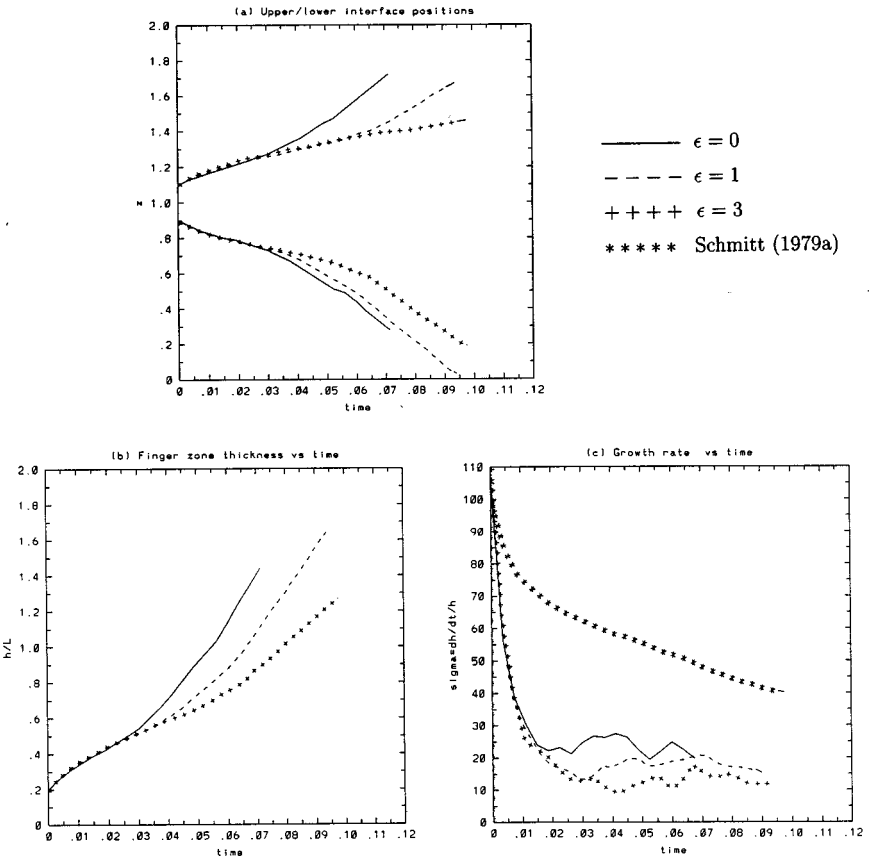

FIG. 4. (a) Positions of the upper and lower mixed-layer/finger interfaces, (b) total finger zone thickness h/L, and (c) nondimensional growth rate $\sigma = h^{-1} dh/dt$ versus time for all experiments.

when the nonlinear term is included. Furthermore, Figs. 3(b) and 3(c) show that the density decreases faster toward the upper interface.

For the initialization, it is opted to fix the local density ratio to 1.8 at the bottom of the finger zone in the present series of simulations. Consequently, the density ratio increases in the upward direction along the finger zone for the nonlinear cases. Alternatively (as suggested by a reviewer), one can choose a nonlinear temperature distribution so as to make the local density ratio the same at the top and the bottom of the interface. Numerical experiments conducted with these initial conditions (not shown) demonstrate that vertical diffusion of temperature takes place faster than the growth of fingers such that the temperature profile becomes linear and the subsequent evolution of the fingers is not substantially different from those presented below.

The growth of the finger instability is depicted in Fig. 4. Figure 4(a) shows the positions of the lower and upper interfaces between the finger zone and the mixed layers for all experiments. The initial development of the interface is the same for all cases, since it is associated with the diffusive adjustment from the initial conditions before the onset of the finger instability. There is then a transition to a faster growth of the interface, indicating the start of the finger instability. For $\epsilon = 0$, this process is identical at the upper and lower interfaces, while for the nonlinear cases, the onset of the finger instability is delayed. Furthermore, there is an offset between the upper and lower interfaces; the transition to fast growth begins earlier at the lower interface, and the growth is faster than at the upper interface. Both trends are consistent with the behaviors discussed above.

Figure 4(b) shows the change of the finger zone thickness in time. Initial diffusive growth ($0 \leqslant t \leqslant 0.02$) is a result of small initial perturbations (Fig. 2), which do not protrude into the reservoirs. The initial adjustment is followed by a rapid growth of the finger zone (for approximately $0.02 < t \leqslant 0.05$). Piacsek and Toomre[6] observed an exponential growth followed by a linear growth in their numerical simulations. A similar transition is captured in the present simulations.

The growth rate $\sigma = h^{-1} dh/dt$ (where h is the thickness of the finger zone) is plotted in Fig. 4(c) for all cases. For reference, the growth rate as calculated from the analytical model of Schmitt[4] is also plotted as a function of the varying temperature gradient. The initial growth rate is predicted well by the formula derived in Schmitt.[4] However, at later stages, the present simulation (i.e., only the case with $\epsilon = 0$ is applicable) departs from the analytical prediction by roughly a factor of 2. This is due to two reasons: (i) Schmitt[4] assumes constant background temperature and salinity gradients, whereas in the present numerical simulations, the mean temperature and salinity gradients are determined in conjunction with the evolution of the fingers. (ii) The z-dependence is neglected in Schmitt[4] as in most analytical models. As it is discussed in Sec. V B, the formation of complex flow structures such as blobs at finger tips and their complicated inter-

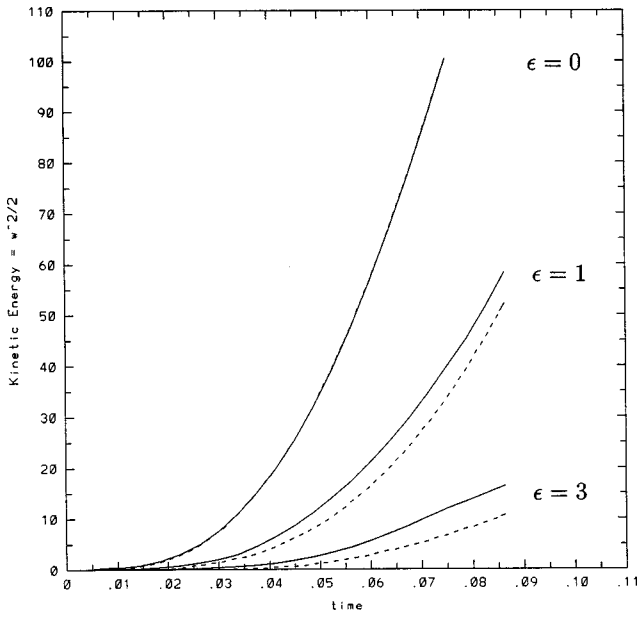

FIG. 5. Vertical kinetic energy $w^2/2$ versus time for all experiments. The solid lines and the dashed lines show the vertical kinetic energy averaged over all descending and ascending fingers, respectively.

action with the reservoirs contribute to the differences from the predictions of the analytical studies. Figure 4(c) indicates that the growth rate is affected by the nonlinearity in the equation of state; the growth rate decreases with increasing nonlinearity parameter ϵ.

The build-up of vertical kinetic energy $w^2/2$ of the fingers throughout the numerical integration is plotted in Fig. 5 [the velocity field is $(u,w)=(-\psi_z,\psi_x)$]. For the linear case, both descending (solid line) and ascending fingers (dashed line) have identical developments in kinetic energy, and the conversion of the potential energy available in the salinity field begins earlier and is faster than in the nonlinear cases. As the nonlinearity parameter ϵ increases, the onset of the finger instability is delayed, the rate of kinetic energy build-up decreases, and the ratio of the kinetic energy of descending over ascending fingers increases.

Salinity, temperature and density fields for all runs are exhibited in Fig. 6 for $t=0.075$, when the numerical integration for the linear case ($\epsilon=0$) is terminated before the finger tips interact with the vertical boundaries of the domain. The most striking element in this figure is the variations in the shapes of salt fingers that are particularly visible in the salinity plots [Figures 6(c), 6(f), 6(i)]. Salinity is preserved along the fingers whereas heat is diffused, making salinity suitable for the visualization of the fingers. For the same reason, the stabilizing effect due to temperature decreases along the fingers, and this leads to an acceleration of the flow along the fingers. The mass within the fingers is conserved because there is insignificant mass exchange between adjacent fingers that maintain a quasi-laminar flow structure. Therefore the thickness of the fingers decreases in the direction of the flow. The finger tips show signs of evolution toward blobs characterized by dipolar vortices. Such structures are generic flow patterns that tend to appear in two-dimensional systems via the self-organization of the flow[16,17]

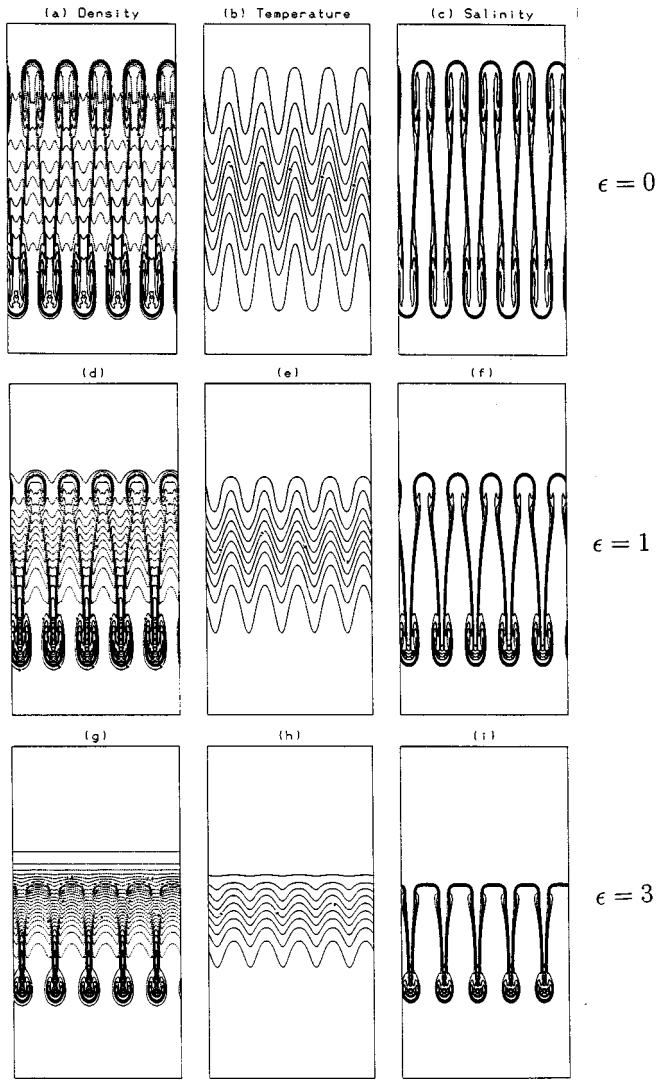

FIG. 6. The density, temperature and salinity fields, respectively, for $\epsilon=0$ (a)–(c), $\epsilon=1$ (d)–(f) and $\epsilon=3$ (g)–(i), at $t=0.075$ (CI=0.1 for density and temperature, and 0.2 for salinity).

and that correspond to the most probable stable equilibrium state maximizing entropy.[18] These blobs also play an important role in fingers reaching a finite amplitude, when blobs regularly detach from the tips of the fingers, keeping the extent of the finger zone at a statistically steady state.[3,9] The present simulations have not reached an equilibrium state (e.g., Fig. 4) and do not display any blob-shedding during the simulation period.

As the nonlinearity parameter ϵ increases, the descending fingers progressively become faster and narrower with respect to the ascending fingers [Figs. 6(f) and 6(i)]. The difference in buoyancy forcing acting initially on the ascending and descending fingers was demonstrated in Sec. II, which indicated faster growth for descending fingers. For the linear case, the evolution of ascending and descending fingers is entirely symmetric [Fig. 6(c)], and it is faster than the nonlinear cases. After simple algebra, it can be shown that the difference between buoyancy forcing acting on the downward-growing fingers in the nonlinear and the linear cases is proportional to

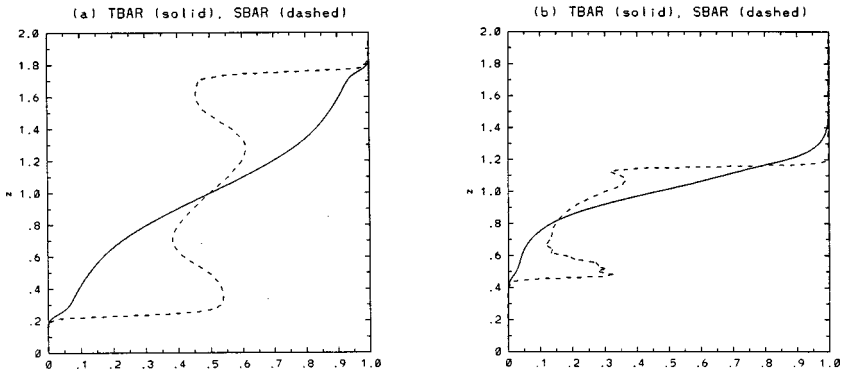

FIG. 7. Background gradients $\overline{T}$ (solid line) and $\overline{S}$ (dashed line) for (a) $\epsilon=0$ and (b) $\epsilon=3$ at $t=0.075$.

$$(\rho_d-\rho_2)^{\text{nonlin}}-(\rho_d-\rho_2)^{\text{lin}} = \gamma[(T_2-T_0)^2-(T_1-\delta T-T_0)^2],$$

where the notations are the same as those in Sec. II. Since $T_1-\delta T>T_2$, the right-hand side of the above expression is negative, indicating stronger buoyancy forcing in the linear case. The numerical results presented in Figs. 4–6 confirm this statement.

B. Vertical distribution of properties

The differences induced by the nonlinearity parameter ϵ on the evolution of the fingers are investigated by analyzing the distribution of the background gradients $\overline{T}(z)$ and $\overline{S}(z)$ (where the overbar indicates the horizontal mean) and of the velocity, temperature, salinity and density perturbations (from the horizontal mean). The perturbations are calculated over the ascending and descending fingers separately, since the nonlinearity leads to an asymmetry in relation to the direction of flow (Fig. 6). Comparisons are made between the linear case ($\epsilon=0$) and the highly nonlinear case ($\epsilon=3$).

1. Mean T and S gradients

Figure 7 illustrates the background gradients averaged over fingers growing in opposing directions at the end of the simulation period ($t=0.075$) for $\epsilon=0$ and $\epsilon=3$. The temperature distribution is dominated by high diffusion. Ascending (descending) fingers warm up (cool down) along the fingers, gradually reaching the reservoir temperatures and leading to an approximately linear gradient in the vertical [Fig. 7(a)]. In the nonlinear case [Fig. 7(b)], the temperature gradient in the lower blob region ($0.3\leqslant z\leqslant 0.7$) is much less than in the interior finger zone due to enhanced diffusion. The $\overline{S}(z)$-distribution in the linear case [Fig. 7(a)] indicates the presence of two distinct regions: an interior gradient region ($0.7\leqslant z\leqslant 1.3$) and blob regions above and below. The large vertical variations in the finger thickness appear to affect the salinity gradients significantly. Below (above) the middle of the domain, thicker ascending (thicker descending) fingers dominate, which tend to reduce (increase) $\overline{S}$. This effect contributes to the positive gradient of $\overline{S}$ in the vertical direction. However, blobs at the tips of ascending (descending) fingers act to decrease (increase) $\overline{S}$ because of the increase in structure thickness. This effect reduces the interior background salinity gradient. The actual density ratio in the interior region is approximately twice the specified value ($R_\rho=1.8$) at this stage. Therefore the presence of bulbous finger tips appears to slow down the growth of the fingers by increasing the density ratio, and may explain part of the deviation from the theoretical estimate [Fig. 4(c)]. Unlike the linear case, the asymmetry in the nonlinear case is clearly evident in Fig. 7(b). The $\overline{S}$ curve shifts toward lower values with respect to the linear case, which indicates the domi-

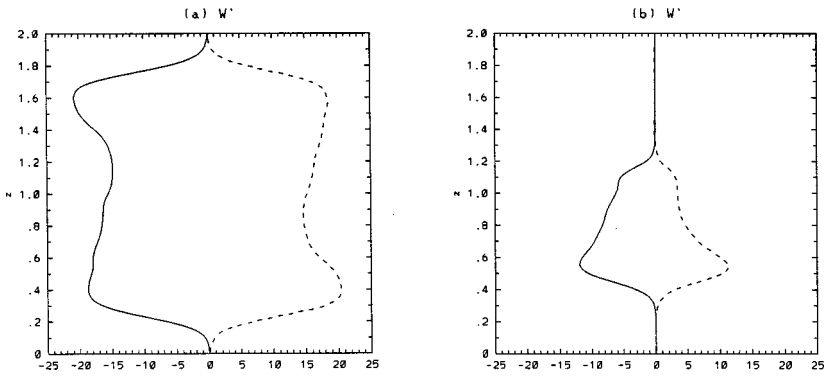

FIG. 8. Vertical velocity w' for (a) $\epsilon=0$ and (b) $\epsilon=3$ at $t=0.075$. The solid (dashed) line denotes the horizontal averages of the perturbations over all the descending (ascending) fingers in the vertical direction.

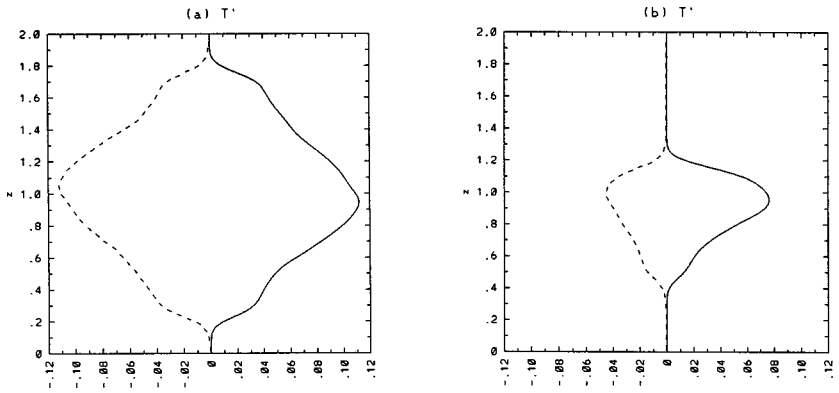

FIG. 9. Temperature perturbation T' for (a) $\epsilon=0$ and (b) $\epsilon=3$ at $t=0.075$. The solid (dashed) line denotes descending (ascending) fingers.

nance of ascending fingers carrying lower S' values over descending fingers (ascending fingers are much thicker than their descending counterparts).

2. Vertical velocity

The distribution of the vertical velocity is depicted in Fig. 8. Since there is no mean vertical motion, $w'=w$. The distribution of w' basically reflects the shape of the fingers as the exchange of mass between the fingers is negligible. Near the entrance region to the fingers [Fig. 8(a)], the vertical velocity is high due to the narrow entrance caused by bulbous finger tips on both sides. The vertical velocity is reduced upon passing the finger tips and increases again due to narrowing of fingers. For descending fingers in the nonlinear case, the entrance velocity is reduced [Fig. 8(b)] because bulbs do not form at the finger tips of the ascending fingers [Fig. 6(i)]. However, the entrainment velocity into the ascending fingers is still large due to the narrow entrance between the bulbous finger tips of sinking fingers. In the finger zone, the vertical velocity in descending fingers is larger than in ascending fingers.

3. Temperature perturbation

The temperature perturbation T' is small near the reservoirs (Fig. 9), because the water parcels entering the fingers have a temperature close to the reservoir temperatures, while the water parcels at the finger tips have already reached the reservoir temperatures due to diffusion along the fingers. For a highly diffusive case, T' would be small and would follow the $\overline{T}$ curve closely. Deviations from the mean gradient therefore measure the dominance of advective over diffusive processes. The magnitude of T' reaches a maximum in the middle of the domain in the linear case [Fig. 9(a)]. For the nonlinear case [Fig. 9(b)], the temperature perturbation T' in ascending fingers is smaller than in descending fingers for two reasons: (1) the geometric factor; ascending fingers are thicker than descending fingers, biasing $\overline{T}$ toward colder temperatures; and (2) the diffusive factor; in the finger zone, the ascending fingers have a slower vertical speed, allowing more time for heat diffusion.

4. Salinity perturbation

Unlike temperature, salinity along the fingers is roughly preserved, and this is reflected by an immediate jump at the finger zone (Fig. 10). The S' distribution is affected by the shape of the fingers. For the linear case [Fig. 10(a)], S' is highest in the middle of the domain ($z=1$) where ascending and descending fingers have the same thickness. S' is slightly less than 0.5 (maximum value) due to the presence of narrow salinity boundary layers. Near the entrance, S' is smaller than in the middle because $\overline{S}$ is higher (lower) for descending (ascending) fingers. In the S' distribution for the nonlinear case [Fig. 10(b)], only the geometric factor plays a role. This effect leads to a higher salinity perturbation in descending fingers, as explained above.

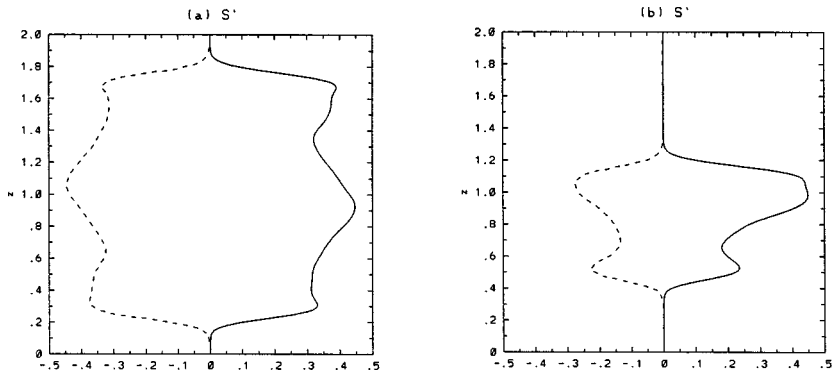

FIG. 10. Salinity perturbation S' for (a) $\epsilon=0$ and (b) $\epsilon=3$ at $t=0.075$. The solid (dashed) line denotes descending (ascending) fingers.

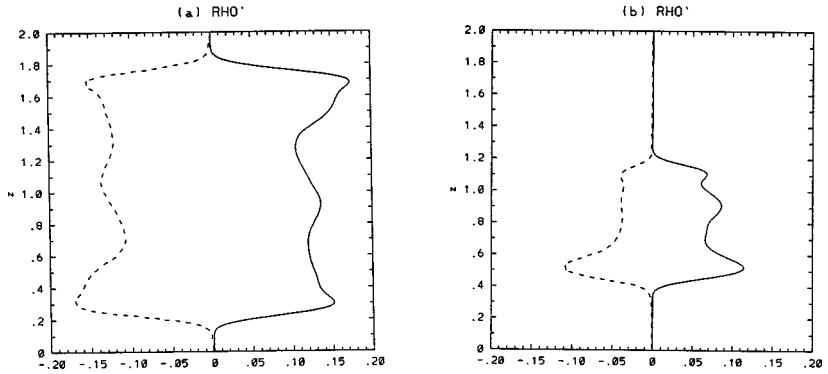

FIG. 11. Density perturbation ρ' for (a) $\epsilon=0$ and (b) $\epsilon=3$ at $t=0.075$. The solid (dashed) line denotes descending (ascending) fingers.

5. Density perturbation

The density-perturbation distribution (Fig. 11) is proportional to the net buoyancy forcing acting on the fluid parcels in the fingers. In the entrance regions, the temperature perturbation is small, and the density perturbation is determined by the salinity perturbation. This leads to a large buoyancy force acting on the fluid parcels entering the fingers [Fig. 11(a)]. For the nonlinear case, the density perturbations in descending fingers are in general larger than in ascending fingers [Fig. 11(b)], resulting in a larger buoyancy force acting on the fluid parcels in the descending fingers. As discussed in Sec. II, this is the cause of the asymmetry between the rising and sinking fingers.

6. Flux ratio

The flux ratio $R_F=\alpha F_T/\beta F_S$, where $F_T=\overline{w'T'}$ and $F_S=\overline{w'S'}$ are the advective heat and salt fluxes, respectively. It is the ratio of the potential energy gained by the temperature field to the potential energy lost by the salinity field. It must be less than unity, since otherwise the system would be gaining energy. The diffusive processes transport heat more rapidly than salt, but since the system is driven by the salt distribution, the fingers transport more salt than heat. Hence, R_F approaches unity when diffusive transport is high and advective transport is small. Lower values of R_F are associated with vigorous finger activity. The values of R_F obtained in laboratory experiments for heat-salt fingers vary considerably, from 0.4 to 0.8, in experiments carried out by Turner,[19] Schmitt,[12] McDougall and Taylor,[20] and Taylor and Buchens.[21]

The flux ratio in our linear experiment at the end of the simulation period ($t=0.075$) is plotted in Fig. 12, averaged over ascending and descending fingers separately. In the linear case [Fig. 12(a)], R_F ranges approximately from 0.35 to 0.5 in the finger zone excluding the blob region. The flux ratios for both ascending and descending fingers for $\epsilon=3$ are exhibited in Fig. 12(b). Lower values of R_F for descending fingers indicate a higher downward flux of density, and are associated with more vigorous finger activity. This is in agreement with our previous results.

VI. SUMMARY AND CONCLUSIONS

The impact of the nonlinearity in the equation of state due to change of the thermal expansion coefficient with temperature on the evolution of double-diffusive fingers is investigated. The initial evolution of the fingers that grow from the interface between two mixed layers in a heat-salt system is considered. We have employed a numerical model integrating the two-dimensional equations of motion for an incompressible, Boussinesq fluid.

An increase in the nondimensional nonlinearity parameter ϵ acts to enhance the buoyancy force acting on the descending fingers with respect to that acting on the ascending fingers, which results in a faster development of descending

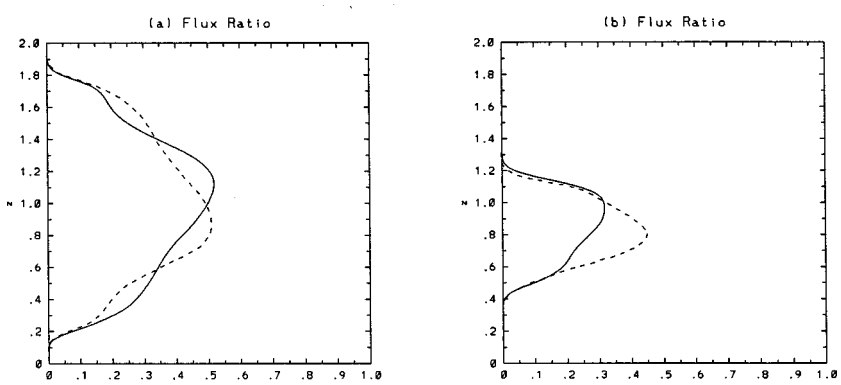

FIG. 12. The flux ratio R_F for (a) $\epsilon=0$ and (b) $\epsilon=3$ at $t=0.075$. The solid (dashed) line marks the horizontal averages over all the descending (ascending) fingers.

fingers than of ascending fingers. Also, the results demonstrate that the descending fingers become narrower than the ascending fingers.

In the present series of simulations, it is shown that the nonlinearity slows down the growth rate of the fingers. Another factor contributing to this result is the initialization choice to fix the actual density ratio to a specified value of density ratio at the bottom of the gradient zone. This prevents any possible gravitational instability at the bottom of the gradient zone, but also leads to slower growth rate for the nonlinear cases since the density ratio for those is higher than that for the linear case. However, experiments conducted with nonlinear initial temperature profile so as to make the local density ratio the same at the top and bottom of the interface do not substantially differ from those presented in this paper. This further substantiates that the dominant factor leading to asymmetric fingers is the nonlinearity in the equation of state rather than asymmetric initial conditions.

The results also indicate high vertical variability along the fingers, which has been disregarded for simplicity in most previous analytical studies. The change in the finger thickness due to the acceleration of the flow along the fingers, as well as the interaction of bulbous finger tips with the reservoirs, play an important role during the initial evolution simulated in the present study. The results indicate that the bulbous finger tips interact with the interior finger zone in such a way that the salinity gradient is reduced, which then causes an increase in the density ratio and decreases the growth rate of the fingers.

We have only focused on the initial evolution of the fingers, with special emphasis on the structure of the individual fingers. The investigation of the finite amplitude behavior of the system consisting of mixed layers and finger interfaces requires a significantly larger domain and a longer integration period (e.g., Özgökmen *et al.*[9]).

ACKNOWLEDGMENTS

The authors wish to thank R. W. Schmitt for inspiring this study. T. M. Özgökmen was supported by the Rosenstiel Post-doctoral Fellowship and O. E. Esenkov by the National Science Foundation under Grant No. OCE-93-14447.

[1] M. E. Stern, ''The 'salt fountain' and thermohaline convection,'' Tellus **12**, 172 (1960).
[2] P. F. Linden, ''On the structure of salt fingers,'' Deep-Sea Res. Oceanogr. Abstr. **20**, 325 (1973).
[3] J. R. Taylor and G. Veronis, ''Experiments on double-diffusive sugar-salt fingers at high stability ratio,'' J. Fluid Mech. **321**, 315 (1996).
[4] R. W. Schmitt, ''The growth rate of super-critical fingers,'' Deep-Sea Res. Oceanogr. Abstr. **26**, 23 (1979).
[5] E. Kunze, ''Limits on growing, finite-length salt fingers: A Richardson number constraint,'' J. Mar. Res. **45**, 533 (1987).
[6] S. Piacsek and J. Toomre, ''Nonlinear evolution and structure of salt fingers,'' in *Marine Turbulence*, edited by J. C. J. Nihoul (Elsevier, Amsterdam, 1980).
[7] C. Y. Shen, ''The evolution of the double-diffusive instability: Salt fingers,'' Phys. Fluids A **1**, 829 (1989).
[8] C. Y. Shen, ''Heat-salt finger fluxes across a density interface,'' Phys. Fluids A **5**, 2633 (1993).
[9] T. M. Özgökmen, O. E. Esenkov, and D. B. Olson, ''A numerical study of layer formation due to fingers in double-diffusive convection in a vertically-bounded domain,'' J. Mar. Res. **56** (2), 463 (1998).
[10] T. J. McDougall, ''Double-diffusive convection with a non-linear equation of state. Part I. The accurate conservation properties in a two-layer system,'' Prog. Oceanogr. **10**, 71 (1981).
[11] T. J. McDougall, ''Double-diffusive convection with a non-linear equation of state. Part II. Laboratory experiments and their interpretation,'' Prog. Oceanogr. **10**, 91 (1981).
[12] R. W. Schmitt, ''Flux measurements at an interface,'' J. Mar. Res. **37**, 419 (1979).
[13] J. Gazdag, ''Time-differencing schemes and transform methods,'' J. Comput. Phys. **20**, 196 (1976).
[14] A. Arakawa, ''Computational design for long-term numerical integration of the equations of fluid motion: Two dimensional incompressible flow. Part I,'' J. Comput. Phys. **1**, 119 (1966).
[15] P. N. Swarztrauber, ''The methods of cyclic reduction, Fourier analysis and FACR algorithm for discrete solution of the Poisson equation an a rectangle,'' SIAM (Soc. Ind. Appl. Math.) Rev. **19**, 490 (1977).
[16] G. R. Flierl, M. E. Stern, and J. A. Whitehead, ''The physical significance of modons: laboratory experiments and general integral constraints,'' Dyn. Atmos. Oceans **7**, 233 (1981).
[17] A. H. Nielsen and J. J. Rasmussen, ''Formation and temporal evolution of the Lamb-dipole,'' Phys. Fluids **9**, 982 (1996).
[18] R. A. Smith, ''Maximization of vortex entropy as an organizing principle in intermittent, decaying, two-dimensional turbulence,'' Phys. Rev. A **43**, 1126 (1991).
[19] J. S. Turner, ''Salt fingers across a density interface,'' Deep-Sea Res. Oceanogr. Abstr. **14**, 599 (1967).
[20] T. J. McDougall and J. R. Taylor, ''Flux measurements across a finger interface at low values of the stability ratio,'' J. Mar. Res. **42**, 1 (1984).
[21] J. R. Taylor and P. Buchens, ''Laboratory experiments on the structure of salt fingers,'' Deep-Sea Res. Oceanogr. Abstr. **36**, 1675 (1989).